



J. Serb. Chem. Soc. 89 (7–8) 997–1009 (2024)
JSCS–5767

***In silico* studies of phycobilins as potential candidates for inhibitors of viral proteins associated with COVID-19**

VESNA B. JOVANOVIĆ¹, MILAN R. NIKOLIĆ^{1#} and SRĐAN Đ. STOJANOVIĆ^{2*}

¹University of Belgrade, Faculty of Chemistry, Department of Biochemistry and Centre of Excellence for Molecular Food Sciences, Belgrade, Serbia and ²University of Belgrade, Institute of Chemistry, Technology and Metallurgy – National institute of the Republic of Serbia, Department of Chemistry, Belgrade, Serbia

(Received 26 March, revised 17 April, accepted 8 May 2024)

Abstract: In this *in silico* study, it was investigated whether phycobilins (phycocyanobilin, phycoerythrobilin and phycourobilin) could be inhibitors of the activity of the main proteins of the SARS-CoV-2 virus. All chromophores exhibited a binding energy value of ≥ -37 kJ mol⁻¹ for PLpro-WT, PLpro-C111S, helicase-ANP binding site, Nsp3-macrodomain, Nsp3-MES site and Nsp10/14-N7-Mtase. Phycocyanobilin showed the highest binding energy of -44.77 kJ mol⁻¹ against the target protein PLpro-C111S. It was found that, apart from the hydrogen bonds and hydrophobic interactions, phycobilins also form electrostatic interactions with the SARS-CoV-2 proteins. The network of non-covalent interactions was found to be important for the stability of the examined virus proteins. All phycobilins have good pharmacokinetic and drug-likeness properties. This study's results suggest that the screened phycobilins could serve as promising drugs for the treatment of COVID-19 with further rigorous validation studies.

Keywords: phycobilins; COVID-19; inhibitors; proteins; *in silico* studies.

INTRODUCTION

The SARS-CoV-2 infection has spread around the world at an extremely high speed, causing a severe medical and humanitarian crisis in almost every region of the world. This virus has been officially linked to severe acute respiratory syndrome coronaviruses (SARS-CoVs) and named severe acute respiratory syndrome coronavirus 2 (SARS-CoV-2) by the International Committee on Taxonomy of Viruses.¹ Coronavirus Disease 2019 (COVID-19) is an infectious respiratory disease caused by SARS-CoV-2, a recently discovered coronavirus strain. Despite advances in vaccine and drug research, there is still a lack of

* Corresponding author. E-mail: srdjanst@chem.bg.ac.rs

Serbian Chemical Society member.

<https://doi.org/10.2298/JSC240326052J>

prophylactic vaccinations and effective antiviral drugs for many viral diseases, including coronavirus infections.^{2,3} Finding effective therapeutic strategies for treating COVID-19 patients has thus become a crucial and urgent task. Different methods can be used for antiviral research to act against SARS-CoV-2. For example, target structural proteins in view to inhibit virus entry in human host cells, looking for functional internal viral protein inhibitors to block its replication or target human receptor for virus entry prevention.^{4–6} Computation docking is an effective strategy and widely used technique for understanding the molecular aspects of proteins and protein–ligand interactions in the drug discovery.^{5,7} Interactions between SARS-CoV-2 proteins have been extensively studied from a biothermodynamic perspective. For example, binding affinities of the spike glycoprotein of various variants of SARS-CoV-2 to the ACE2 receptor have been discussed.^{8–10}

Natural products with antimicrobial and antiviral properties are of great interest to scientists to study their effectiveness in combating COVID-19.¹¹ Medicines based on natural phytochemicals are gaining traction in modern healthcare due to their lower toxicity, effective health benefits and potential use in connection with existing therapies becoming increasingly important. Marine products are known to serve as a seemingly limitless bioresource to combat pathogenic microbes and cancers.¹² Several literature studies have reported the antiviral properties of phytochemicals against CoVs and other viruses.^{13,14} Kumar *et al.*¹⁵ used molecular docking and molecular dynamics simulations to screen effective compounds from purple nutsedge (*Cyperus rotundus*) against the main protease (Mpro) of SARS-CoV-2. Silva *et al.*¹⁶ investigated the pharmacokinetic and toxicological properties of molecules in a natural product data-base of the Brazilian semiarid region and performed location prediction and drug-ability analysis on SARS-CoV-2 Mpro. Gupta *et al.*¹⁷ screened more than 53,500 bioactive natural molecules from six different natural product databases to identify effective molecules against Mpro. Li *et al.*¹⁸ used ensemble and cooperative docking and molecular simulations to investigate possible interactions of more than 600 compounds from a herbal drug with eight SARS-CoV-2 proteins, including spike protein, nucleocapsid protein, Mpro and papain-like protease, RNA-dependent RNA polymerase (RdRp), nonstructural protein 3 (Nsp3), and cat/human angiotensin-converting enzyme 2. Pendyala and Patras¹⁹ showed that phycocyanobilins showed high binding affinity for the SARS-CoV-2 Mpro and RdRp *in silico* molecular docking studies. Despite the challenges, it is clear that marine organisms represent a promising avenue for future pharmacological interventions.²⁰

The results of our study prompted us to take further steps, primarily examining all proteins and binding profiles with phycobilins available in the COVID-19 docking server. Phycobilins are open-chain light-trapping tetrapyrrole pigments found in cyanobacteria (blue phycocyanobilin) and red algae (red phycoerythron-

bilin and orange phycourobilin). They are covalently bound to phycobiliproteins *via* a thioether bond and are carriers of the powerful biological activities of these fluorescent water-soluble proteins with new pharmaceutical potential.²¹

The present study aimed to identify the most relevant antiviral SARS-CoV-2 phycobilin molecules through docking and *in silico* toxicity assessment. We report natural phycobilins as potent broad-spectrum natural inhibitory compounds against major SARS-CoV-2-associated proteins *via* an *in silico* approach.

EXPERIMENTAL

Molecular docking and visualization

To investigate the affinity of phycobilins toward SARS-CoV-2 virus' receptors, molecular docking calculations were carried out using COVID-19 Docking Server 2.0 (nCoVdocking2).²² A new docking server, nCoVdocking2 was constructed to predict the binding modes between the wild type and mutants of SARS-CoV-2 therapeutic targets and their potential ligands. AutoDock Vina²³ is used as the docking engine for small molecule docking. AutoDock Vina is upgraded to the latest version 1.2.0,²⁴ on the new server. Open Babel was used for format transformation or 3D coordinate generation for the uploaded files.²⁵ The docking box is defined as the center of native ligand coordinates with dimensions of 30 Å×30 Å×30 Å to include residues of the entire cavity. Homology-modeled structures are defined according to the information of active sites or binding sites of its homologs of SARS-CoV. The MGLTools was used to add hydrogens and prepare pdbqt files for proteins and ligands. All the parameters were set as default, and we chose the exhaustiveness value option as 12. The higher level of exhaustiveness parameter is considered to provide more precise docking results and longer computational time. We used all proteins provided by this server (Table I). The input 3D sdf ligand files of selected phycobilins (phycocyanobilin, phycoerythrobilin and phycourobilin) were retrieved from PubChem²⁶ database (<https://pubchem.ncbi.nlm.nih.gov/>) and uploaded to COVID-19 Docking Server 2.0. The docked receptor and ligand interactions were visualized using Biovia Discovery Studio Visualizer.²⁷

Non-covalent interaction analysis

The docked receptor and ligand interactions were analyzed and visualized using Biovia Discovery Studio Visualizer²⁷ with default-specific criteria and geometrical feature settings (these criteria and settings are provided in the Supplementary material to this paper).

Physicochemical, pharmacokinetic, drug-likeness and medicinal chemistry properties

Physicochemical, pharmacokinetic, drug-likeness and medicinal chemistry properties were predicted for the phycobilins using the SwissADME server.²⁸ The SMILES format of the phycobilins was retrieved from the PubChem database and used as input for the SwissADME server.

RESULTS AND DISCUSSION

The first part of this work focuses on evaluating anti-SARS-CoV-2 activity by docking phycobilin compounds. The second part of the article deals with an *in silico* study on the toxicity of the selected molecules.

Molecular docking studies

Molecular docking simulations were performed to determine the binding affinities between the phycobilins and the target SARS-CoV-2 protein sites and to identify the molecular interactions that play a key role in binding. COVID-19 Docking Server, an online meta server, was built to elaborate on the SARS-CoV-2 target–ligand interactions. Structures of proteins involved in the virus life cycle were established based on the homologs of coronavirus. The binding mode and affinity between estimated molecules and target protein can be deduced through this server. Based on the above, all the phycobilins were submitted to the COVID-19 Docking Server to unveil their interfering capacity in the life cycle of the SARS-CoV-2 virus. Docking results of all compounds in difference proteins expressing as score value (kJ mol^{-1}) and RF score value are presented in Table I. They are associated with the top-ranked poses (best models of studied complexes). Score value below or equal to -33 kJ mol^{-1} demonstrates a significant strength of interactions between small molecules and proteins; the lower the score value, the stronger the interaction. The distribution frequency of binding energy score among the phycobilins and SARS-CoV-2 proteins varies between -21 and -45 kJ mol^{-1} .

In all the simulated ligand–protein docking model, among all targets, PLpro-WT, PLpro-C111S, Helicase-ANP binding site, Nsp3-macrodomein, Nsp3-MES site and Nsp10/14-N7-Mtase displayed higher score than all other proteins. Papain-like protease (PLpro) is an interesting antiviral target because it is essential for replicating coronaviruses.²⁹ In addition, as a consequence of the alterations present in the genome of SARS-CoV-2, the PLpro is now well-equipped to cleave the ubiquitin-like interferon-stimulated gene 15 protein,²⁹ thereby evading the host's innate immune responses. The docking scores of the other proteins, except for Nsp10-nsp10-14 and Nsp10-nsp10-16, were lower than -30 kJ mol^{-1} and also exhibited notable affinities, implying these proteins may be potent targets for inhibition of SARS-CoV-2. Among the phycobilins, the results revealed that the affinities of phycocyanobilin for PLpro-C111S, Helicase-ANP binding site, RdRp-RTP site and Nsp3-macrodomein, Nsp10/14-N7-Mtase was highest, indicating that phycocyanobilin was the main antiviral active component. The results show phycocyanobilin docked with the best score with a binding energy of $-44.77 \text{ kJ mol}^{-1}$. It is interesting to note that phycoerythrobilin showed higher affinity for non-structural proteins: Nsp10/16-MGP site, Nsp10/16-SAM site, Nsp10/16-GTA site, Nsp10/14-N7-Mtase and Nsp10/14-chapso site than other phycobilins and the origin ligands. The difference arises from the higher number of non-covalent interactions in phycoerythrobilin–non-structural protein interfaces; the interplay between interactions may exist. This should also be taken into account when determining binding affinity. Therefore, these phycobilins could be potent inhibitors of SARS-CoV-2 targets. Non-structural proteins (Nsp10-nsp10-

-14 and Nsp10-nsp10-16) have shown the weakest binding energy among the proteins studied, possibly due to the dominance of hydrophobic residues involved in the binding pocket with phycobilins. The results of molecular docking scoring were consistent with those of Mpro and PLpro target proteins previously reported.¹⁹

TABLE I. Covid-19 docking server results of phycobilins; *SV* – score value; *RF SV* – RF score value

Protein	Phycocyanobilin		Phycourobilin		Phycocyanobilin	
	<i>SV</i> kJ mol ⁻¹	<i>RF SV</i> pKd	<i>SV</i> kJ mol ⁻¹	<i>RF SV</i> pKd	<i>SV</i> kJ mol ⁻¹	<i>RF SV</i> pKd
Nsp3-macrodomein (5RSF)	-37.24	7.37	-36.82	7.05	-39.33	7.51
Nsp3-ADP ribose phosphatase (6W6Y)	-33.05	7.00	-32.22	6.65	-34.73	7.30
Nsp3-MES site (6W6Y)	-34.73	6.79	-39.33	7.34	-39.33	7.62
PLpro-WT (7RZC)	-39.75	7.97	-43.93	7.86	-43.10	7.90
PLpro-C111S (7SQE)	-42.26	7.82	-39.33	7.84	-44.77	8.09
Mpro-WT (7SI9)	-33.89	7.12	-34.31	7.15	-35.15	7.14
Nsp9-FR6 bound (7KRI)	-29.71	6.30	-28.87	6.09	-29.71	6.26
Nsp9-oridonin bound (7N3K)	-37.24	7.81	-37.66	7.64	-38.49	7.52
Nsp10-nsp10-14 (7ORR)	-27.61	6.08	-23.85	5.76	-25.94	5.77
Nsp10-nsp10-16 (7ORU)	-24.69	6.09	-20.82	5.76	-26.78	6.05
RdRp-RTP site (7BV2)	-40.58	7.88	-40.17	7.93	-41.00	7.90
RdRp-RNA site (7D4F)	-31.79	6.76	-29.71	6.74	-28.45	6.40
Helicase-ANP binding site (7NN0)	-37.66	7.33	-38.07	7.77	-41.00	7.43
Helicase-fragment binding site (5RML)	-36.82	7.29	-35.15	7.08	-28.45	7.37
Nsp10/14-chapso site (7N0D)	-38.91	7.26	-35.56	7.15	-36.82	7.30
Nsp10/14-ExoN (7N0D)	-30.54	6.81	-32.22	6.87	-30.54	7.62
Nsp10/14-N7-Mtase (7N0D)	-43.51	7.79	-40.58	8.02	-41.00	7.64
Nsp15-WT (7K1L)	-30.96	6.53	-30.54	6.33	-32.22	6.44
Nsp10/16-MGP site (6WVN)	-39.33	7.45	-36.41	6.96	-36.82	7.43
Nsp10/16-SAM site (6W4H)	-39.33	7.49	-36.82	7.10	-36.82	7.46
Nsp10/16-GTA site (6WVN)	-38.91	7.34	-36.82	7.09	-35.98	7.44
Nprotein-NCB site (MODEL)	-34.73	7.24	-35.15	7.26	-33.05	7.54

Binding profile of SARS-CoV-2 associated proteins with the phycobilins

To better understand binding affinity, we also listed the binding profile of the SARS-CoV-2 associated proteins with the relevant phycobilins mentioned above, molecular interaction types, and their properties in Table II.

The interaction prediction using Discovery Studio Visualizer software revealed that phycobilins could have various interactions. While analyzing the interaction profile, it was found that, apart from the hydrogen bonds and hydrophobic

interactions, which were considered the most common type of protein–ligand interactions,³⁰ phycobilins also form electrostatic interactions with the SARS-CoV-2 proteins. Ion pairs play an important role in the stabilization of protein structures. Electrostatic interactions are infrequent among protein–ligand interfaces (Table II). Many of interfaces did not form electrostatic interactions, while the largest number of electrostatic interactions in an interface was five (Phycocyanobilin–PLpro-C111S). From Fig. 1, the types of molecular interactions and the interacting residues of the PLpro-C111S chains can be clearly seen.

TABLE II. Interaction profiles between SARS-CoV-2 associated proteins and the tested phycobilins

Protein	Phycobilin											
	Phycoerythrobilin				Phycourobilin				Phycocyanobilin			
	N _{HB} ^a	N _{ES} ^b	N _{HP} ^c	N _O ^d	N _{HB}	N _{ES}	N _{HP}	N _O	N _{HB}	N _{ES}	N _{HP}	N _O
Nsp3-macrodomein (5RSF)	3	–	7	–	4	–	4	–	2	–	8	–
Nsp3-ADP ribose phosphatase (6W6Y)	4	–	8	–	2	–	3	–	8	–	7	–
Nsp3-MES site (6W6Y)	4	–	6	–	4	–	6	–	5	–	8	–
PLpro-WT (7RZC)	7	1	5	–	2	1	7	–	3	3	4	–
PLpro-C111S (7SQE)	7	1	3	–	5	2	2	–	5	5	3	–
Mpro-WT (7S19)	5	–	–	2	2	–	2	1	6	4	2	–
Nsp9-FR6 bound (7KRI)	6	–	4	–	3	–	6	–	5	–	3	–
Nsp9-oridonin bound (7N3K)	5	1	5	–	4	1	2	–	2	1	4	–
Nsp10-nsp10-14 (7ORR)	4	–	3	–	2	–	4	–	3	–	3	–
Nsp10-nsp10-16 (7ORU)	4	–	3	–	4	1	–	–	6	1	–	–
RdRp-RTP site (7BV2)	4	–	3	–	7	–	4	–	6	4	3	–
RdRp-RNA site (7D4F)	7	–	4	–	2	–	3	–	5	–	3	–
Helicase-ANP binding site (7NN0)	8	–	5	–	8	–	3	–	6	2	1	–
Helicase-Fragment binding site (5RML)	6	1	6	–	5	1	5	–	9	1	5	–
Nsp10/14-chapso site (7N0D)	2	–	8	–	1	–	4	–	2	–	4	–
Nsp10/14-ExoN (7N0D)	5	–	2	1	6	1	–	1	3	5	3	2
Nsp10/14-N7-Mtase (7N0D)	7	–	3	–	9	–	3	–	6	1	5	–
Nsp15-WT (7K1L)	7	1	5	–	2	1	4	–	7	2	4	–
Nsp10/16-MGP site (6WVN)	6	–	4	–	10	–	2	–	6	2	3	–
Nsp10/16-SAM site (6W4H)	5	–	4	–	9	–	2	–	8	–	3	–
Nsp10/16-GTA site (6WVN)	7	–	3	–	11	–	2	–	6	–	3	–
Nprotein-NCB site (MODEL)	2	–	5	–	4	1	6	–	3	3	7	–

^aNumber of hydrogen bonds; ^bnumber of electrostatic interactions; ^cnumber of hydrophobic interactions; ^dnumber of other interactions

As shown, phycocyanobilin interacts with the papain-like protease (PLpro-C111S) through B:Arg166:NH2, B:Glu167:OE1, C:Asp164:OD1, C:Glu167:OE1 and C:Tyr264 *via* electrostatic interactions. Additionally, phycocyanobilin makes

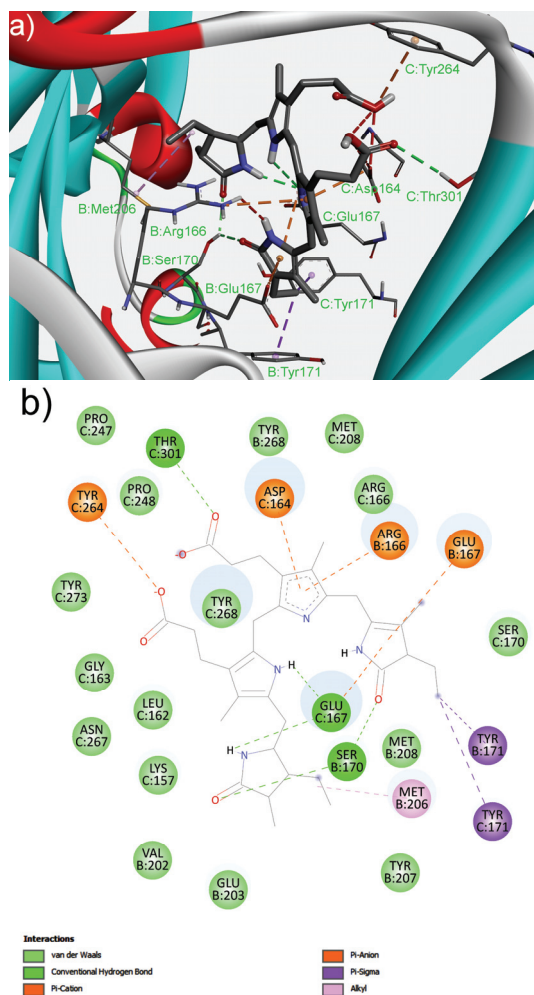


Fig. 1. Details of the strongest binding affinity; $-44.77 \text{ kJ mol}^{-1}$ (phycocyanobilin-PLpro-C111S (7SQE)): a) 3D view and b) 2D view of interaction profile.

five hydrogen bonds (B:Ser170:HG, C:Glu167:OE1 and C:Thr301:HG1) and three hydrophobic interactions (B:Tyr171, B:Met206 and C:Tyr171). The specific arrangement or connectivity of protein clusters could significantly influence their structural stability.³¹ A donor group (HG) from B:Ser170 (PLpro-C111S) interact with two acceptor groups of phycocyanobilin simultaneously. In addition, C:Glu167 makes two hydrogen bonds as an acceptor with phycocyanobilin. This result indicates that these residues are crucial in binding phycocyanobilin and the PLpro enzyme. Hydrogen bonds with multiple donors (acceptor furcation) and multiple acceptors (donor furcation) are common in protein structures. These arrangements might add more stability and play an important role in understanding the 3D structure of protein–ligand complexes.³¹ Here, although RdRp-RNA site has such a large number of hydrogen bond interactions (non-

-multiple), the low binding affinity of the RdRp-RNA site can be attributed to the relatively lower electrostatic and hydrophobic interactions of the RdRp-RNA site compared to other proteins.

The analysis shows that around 45 % of the dataset's total interactions are involved in forming multiple non-covalent interactions. An illustrative example is shown in Fig. 1 that B:Ser170, C:Aasp164 and C:Glu167 form multiple interactions. Another additional feature is the observed additive property of these interactions, showing an effect on the strength of the host-guest system.³¹

As for the non-structural proteins (Nsp10-nsp10-14 and Nsp10-nsp10-16), docking results show the lowest scores between -21 and -27 kJ mol⁻¹, possibly due to the dominance of hydrophobic residues involved in the binding pocket with phycobilins (Fig. 2a). While analyzing the interaction profile of phycocourobilin-Nsp10-nsp10-14 complex (Fig. 2b), it was found that five amino acids such as A:Phe16, A:Ala20, A:Lys25, A:Ala26 and A:Tyr30 were involved in the formation of two hydrogen bonds and four hydrophobic interactions.

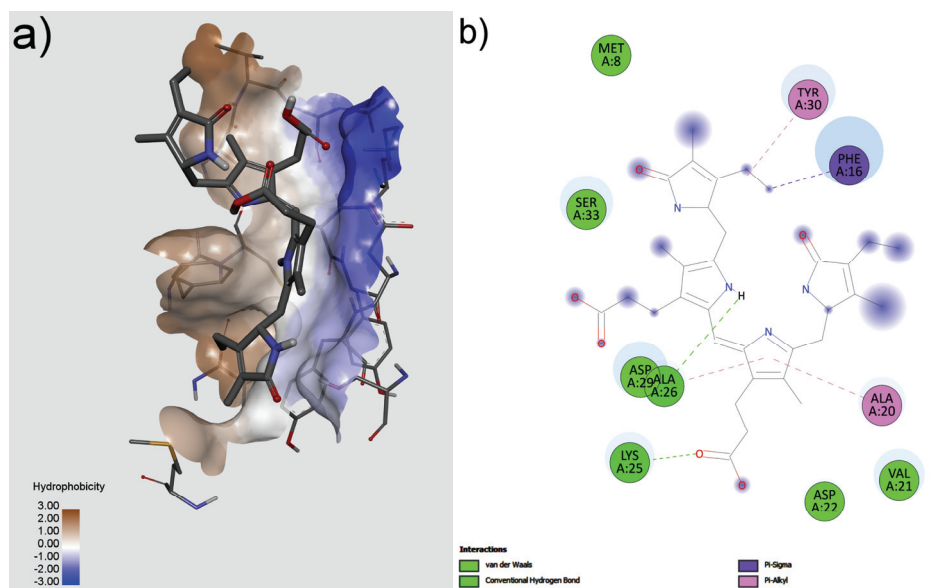


Fig. 2. Details of the weakest binding affinity; -23.85 kJ mol⁻¹ (phycocourobilin-Nsp10-nsp10-14 (7ORR)): a) 3D hydrophobicity view of binding pocket and b) 2D view of interaction profile.

Physiochemical, pharmacokinetic and drug-likeness properties of phycobilins

The ADME (absorption, distribution, metabolism, and excretion) properties of the compounds allow drug developers to understand the reliability and efficacy of a drug candidate compound, accelerating the timeline for the new drug submission process to the Food and Drug Administration (FDA). Therefore, after

docking assays and binding interaction analysis, an *in silico* toxicity study was conducted on the phycobilins with the SwissADME tool (Table III).

TABLE III. Drug-likeness analysis of the phycobilins obtained with SwissADME

Physicochemical property	Phycoerythrobilin	Phycourobilin	Phycocyanobilin
<i>MW</i> / g mol ⁻¹	586.68	590.71	586.68
H-bond acceptors	7	7	7
H-bond donors	5	5	5
<i>TPSA</i> / Å ²	164.71	160.95	164.71
Lipophilicity			
iLOGP	3.81	3.98	3.52
Water solubility			
Log <i>S</i> (ESOL)	-4.38	-3.71	-4.55
Solubility, mg mL ⁻¹	2.45e-02	1.16e-01	1.67e-02
Solubility, mol L ⁻¹	4.18e-05	1.96e-04	2.85e-05
Class	Moderately soluble	Soluble	Moderately soluble
Pharmacokinetics			
GI absorption	Low	Low	Low
BBB permeability	No	No	No
Druglikeness			
Lipinski #violations	1: <i>MW</i> > 500	1: <i>MW</i> > 500	1: <i>MW</i> > 500
Veber #violations	2: Rotors > 10, <i>TPSA</i> > 140	2: Rotors > 10, <i>TPSA</i> > 140	1: <i>TPSA</i> > 140
Bioavailability Score	0.11	0.11	0.11
Medicinal chemistry			
PAINS #alerts	0 alert	0 alert	0 alert
Brenk #alerts	0 alert	0 alert	0 alert
Leadlikeness	No; 2 violations: <i>MW</i> > 350, Rotors > 7	No; 2 violations: <i>MW</i> > 350, Rotors > 7	No; 2 violations: <i>MW</i> > 350, Rotors > 7
Synthetic accessibility	6.09	6.25	6.11

All the screened phycobilins were found to have little violation in the Lipinski rule of 5 (1 violation: *MW* > 500), and it was believed to be effective despite of a few violations. Out of the three compounds, phycourobilin is water soluble, while the others are moderately soluble. While checking the pharmacokinetic profile, it was noted that all compounds were ineffective in crossing the blood brain barrier, so no toxic chemicals crossed it. All the candidates were predicted to be absorbed by the gastrointestinal tract but at a low level. While analyzing medicinal chemistry, it was noted that all phycobilins do not present any resemblance to PAINS and Brenk alerts. It was compelling to note that all the compounds screened were safe as they were non-carcinogenic and non-toxic by nature. Other properties, such as pharmacokinetic, physicochemical and drug-

-likeness properties, are mentioned in Table III. Combined with their docking results, these candidates seem strongly relevant to the search for natural agents to fight against SARS-CoV-2, similar to other marine-derived antiviral compounds.³²

CONCLUSION

The present study considered molecular docking on selected phycobilins submitted to SARS-CoV-2 docking server. The primary purpose of the present paper was to test their ability to inhibit SARS-CoV-2 associated main proteins *via an in silico* approach. In the second part, an *in silico* toxicity analysis was conducted to assess the safety of selected compounds. This study finding revealed that phycobilins had shown high binding energy against PLpro-WT, PLpro-C111S, helicase-ANP binding site, Nsp3-macrodomain, Nsp3-MES site and Nsp10/14-N7-Mtase in the range from -37 to -45 kJ mol⁻¹. The interaction profile revealed that phycobilins could have various interactions (electrostatic, hydrophobic and hydrogen bonds). The strong binding affinity can be attributed to phycobilins' relatively higher electrostatic and hydrophobic interactions with some SARS-CoV-2 proteins. From the results, it can be underlined that around 45 % of the total interacting residues in the dataset are involved in forming of multiple interactions, which might add more stability to the phycobilin–SARS-CoV-2 complex. All phycobilins have good pharmacokinetic and drug-likeness properties. Therefore, all the compounds screened were safe as they were naturally non-carcinogenic and non-toxic. Based on the results obtained, phycobilins can be considered inhibitors against the important viral proteins of SARS-CoV-2. They could serve as potential drugs to treat COVID-19 with further validation studies.

SUPPLEMENTARY MATERIAL

Additional data and information are available electronically at the pages of journal website: <https://www.shd-pub.org.rs/index.php/JSCS/article/view/12867>, or from the corresponding author on request.

Acknowledgement. This research has been financially supported by the Ministry of Science, Technological Development and Innovation of Republic of Serbia (Contract No: 451-03-66/2024-03/200026 and 451-03-66/2024-03/200168).

ИЗВОД

IN SILICO СТУДИЈЕ ФИКОБИЛИНА КАО МОГУЋИХ КАНДИДАТА ЗА ИНХИБИТОРЕ ВИРУСНИХ ПРОТЕИНА ПОВЕЗАНИХ СА COVID-19

ВЕСНА Б. ЈОВАНОВИЋ¹, МИЛАН Р. НИКОЛИЋ¹ и СРЂАН Ђ. СТОЈАНОВИЋ²

¹Универзитет у Београду, Хемијски факултет, Катедра за биохемију и Центар изузетних вредности за молекуларне науке о храни, Београд и ²Универзитет у Београду, Институт за хемију, технологију и металургију, Центар за хемију, Институт од националног значаја за Републику Србију, Београд

У овој *in silico* студији испитано је да ли би фикобилини (фикоцијанобилин, фикоеритробилин и фикоуробилин) могли бити инхибитори активности главних протеина SARS-CoV-2 вируса. Све хромофоре су показале вредност енергије везивања ≥ -37 kJ mol⁻¹ према PLpro-WT, PLpro-C111S, хеликаза-ANP везујућем месту, Nsp3-макродомену, Nsp3-MES месту и Nsp10/14-N7-Mt-ази. Фикоцијанобилин је показао највећу енергију везивања, од $-44,77$ kJ mol⁻¹, за циљни протеин PLpro-C111S. Утврђено је да, осим водоничних веза и хидрофобних интеракција, фикобилини формирају и електростатичке интеракције са SARS-CoV-2 протеинима. Пронађена је мрежа нековалентних интеракција важна за стабилност испитаних вирусних протеина. Сви фикобилини су показали обећавајућа фармакокинетичка својства и карактеристике сличне лековима. Резултати ове студије сугеришу да би, уз додатна ригорозна валидациона испитивања, анализирани фикобилини могли да послуже као обећавајући лекови за COVID-19.

(Примљено 26. марта, ревидирано 17. априла, прихваћено 8. маја 2024)

REFERENCES

1. A. E. Gorbalenya, S. C. Baker, R. S. Baric, R. J. de Groot, C. Drosten, A. A. Gulyaeva, B. L. Haagmans, C. Lauber, A. M. Leontovich, B. W. Neuman, D. Penzar, S. Perlman, L. L. M. Poon, D. V. Samborskiy, I. A. Sidorov, I. Sola, J. Ziebuhr, *Nat. Microbiol.* **5** (2020) 536 (<https://doi.org/10.1038/s41564-020-0695-z>)
2. S. Aboul-Fotouh, A. N. Mahmoud, E. M. Elnahas, M. Z. Habib, S. M. Abdelraouf, *Virol. J.* **20** (2023) 241 (<https://doi.org/10.1186/s12985-023-02210-z>)
3. A. von Delft, M. D. Hall, A. D. Kwong, L. A. Purcell, K. S. Saikatendu, U. Schmitz, J. A. Tallarico, A. A. Lee, *Nat. Rev. Drug Discov.* **22** (2023) 585 (<https://doi.org/10.1038/s41573-023-00692-8>)
4. T. F. Aiello, C. Garcia-Vidal, A. Soriano, *Rev. Esp. Quimioter.* **35** (2022) 10 (<https://doi.org/10.37201/req/s03.03.2022>)
5. C. C. Chang, H. J. Hsu, T. Y. Wu, J. W. Liou, *Tzu Chi Med. J.* **34** (2022) 276 (https://doi.org/10.4103/tcmj.tcmj_318_21)
6. D. Saxena, L. Batra, S. K. Verma, *Pathogens* **12** (2023) 823 (<https://doi.org/10.3390/pathogens12060823>)
7. M. S. Murgueitio, M. Bermudez, J. Mortier, G. Wolber, *Drug Discov. Today Technol.* **9** (2012) e219 (<https://doi.org/10.1016/j.ddtec.2012.07.009>)
8. P. Gale, *Microb. Risk Anal.* **21** (2022) 100198 (<https://doi.org/10.1016/j.mran.2020.100140>)
9. M. E. Popović, G. Šekularac, M. Popović, *Microb. Risk Anal.* **26** (2024) 100290 (<https://doi.org/10.1016/j.mran.2024.100290>)
10. M. Popović, M. Stevanović, M. Mihailović, *J. Serb. Chem. Soc.* **89** (2024) 305 (<https://doi.org/10.2298/JSC240119019P>)

11. C. H. Kim, *Front. Pharmacol.* **12** (2021) 590509 (<https://doi.org/10.3389/fphar.2021.590509>)
12. M. M. Rahman, M. R. Islam, S. Shohag, M. E. Hossain, M. Shah, S. K. Shuvo, H. Khan, M. A. R. Chowdhury, I. J. Bulbul, M. S. Hossain, S. Sultana, M. Ahmed, M. F. Akhtar, A. Saleem, M. H. Rahman, *Environ. Sci. Pollut. Res. Int.* **29** (2022) 46527 (<https://doi.org/10.1007/s11356-022-20328-5>)
13. R. Ghildiyal, V. Prakash, V. K. Chaudhary, V. Gupta, R. Gabrani, Phytochemicals as Antiviral Agents: Recent Updates. in M. K. Swamy (eds) *Plant-derived Bioactives: Production, Properties and Therapeutic Applications*. Singapore: Springer Singapore, 2020:279 (https://doi.org/10.1007/978-981-15-1761-7_12)
14. J. S. Mani, J. B. Johnson, J. C. Steel, D. A. Broszczak, P. M. Neilsen, K. B. Walsh, M. Naiker, *Virus Res.* **284** (2020) 197989 (<https://doi.org/10.1016/j.virusres.2020.197989>)
15. S. B. Kumar, S. Krishna, S. Pradeep, D. E. Mathews, R. Pattabiraman, M. Murahari, T. P. K. Murthy, *Comput. Biol. Med.* **134** (2021) 104524 (<https://doi.org/10.1016/j.compbiomed.2021.104524>)
16. R. C. Silva, H. F. Freitas, J. n. M. Campos, N. M. Kimani, C. H. T. P. Silva, R. S. Borges, S. S. R. Pita, C. B. R. Santos, *Int. J. Mol. Sci.* **22** (2021) 11739 (<https://doi.org/10.3390/ijms222111739>)
17. S. S. Gupta, A. Kumar, R. Shankar, U. Sharma, *J. Mol. Graph. Model.* **106** (2021) 107916 (<https://doi.org/10.1016%2Fj.jmkgm.2021.107916>)
18. J. Li, K. T. McKay, J. M. Remington, S. T. Schneebeli, *Sci. Rep.* **11** (2021) 16307 (<https://doi.org/10.1038/s41598-021-95826-6>)
19. B. Pendyala, A. Patras, C. Dash, *Front Microbiol.* **12** (2021) 645713 (<https://doi.org/10.3389/fmicb.2021.645713>)
20. S. Geahchan, H. Ehrlich, M. A. Rahman, *Marine Drugs* **19** (2021) 409 (<https://doi.org/10.3390/md19080409>)
21. L. Tounsi, H. B. Hlima, F. Hentati, O. Hentati, H. Derbel, P. Michaud, S. Abdelkafi, *Mar. Drugs* **21** (2023) 440 (<https://doi.org/10.3390/md21080440>)
22. K. Liu, X. Lu, H. Shi, X. Xu, R. Kong, S. Chang, *Nucleic Acids Res.* **51** (2023) W365 (<https://doi.org/10.1093/nar/gkad414>)
23. O. Trott, A. J. Olson, *J. Comput. Chem.* **31** (2010) 455 (<https://doi.org/10.1002/jcc.21334>)
24. J. Eberhardt, D. Santos-Martins, A. F. Tillack, S. Forli, *J. Chem. Inf. Model.* **61** (2021) 3891 (<https://doi.org/10.1021/acs.jcim.1c00203>)
25. N. M. O'Boyle, M. Banck, C. A. James, C. Morley, T. Vandermeersch, G. R. Hutchison, *J. Cheminformatics.* **3** (2011) 33 (<https://doi.org/10.1186/1758-2946-3-33>)
26. S. Kim, J. Chen, T. Cheng, A. Gindulyte, J. He, S. He, Q. Li, B. A. Shoemaker, P. A. Thiessen, B. Yu, L. Zaslavsky, J. Zhang, E. E. Bolton, *Nucleic Acids Res.* **51** (2023) D1373-D1380 (<https://doi.org/10.1093/nar/gkac956>)
27. Biovia, D.S. (2021) Discovery Studio Visualizer. San Diego.
28. A. Daina, O. Michielin, V. Zoete, *Sci. Rep.* **7** (2017) 42717 (<https://doi.org/10.1038/srep42717>)
29. D. Shin, R. Mukherjee, D. Grewe, D. Bojkova, K. Baek, A. Bhattacharya, L. Schulz, M. Widera, A. R. Mehdipour, G. Tascher, P. P. Geurink, A. Wilhelm, G. van der Heden van Noort, H. Ovaa, S. Müller, K. P. Knobeloch, K. Rajalingam, B. A. Schulman, J. Cinatl, G. Hummer, S. Ciesek, I. Dikic, *Nature* **587** (2020) 657 (<https://doi.org/10.1038/s41586-020-2601-5>)

30. R. Ferreira de Freitas, M. Schapira, *Med. Chem. Commun.* **8** (2017) 1970
(<https://doi.org/10.1039/C7MD00381A>)
31. A. S. Mahadevi, G. N. Sastry, *Chem. Rev.* **116** (2016) 2775
(<https://doi.org/10.1021/cr500344e>)
32. R. Singh, N. Chauhan, M. Kuddus, *Environ. Sci. Pollut. Res. Int.* **28** (2021) 52798
(<https://doi.org/10.1007/s11356-021-16104-6>).